

Influence of the multiplicity of the roots on the basins of attraction of Newton's method ^{*†‡}

José Manuel Gutiérrez Jiménez

Luis Javier Hernández Paricio

Miguel Marañón Grandes

María Teresa Rivas Rodríguez

Departamento de Matemáticas y Computación,
Universidad de La Rioja, c/Luis de Ulloa s/n, 26004 Logroño. Spain

jmguti@unirioja.es luis-javier.hernandez@unirioja.es
miguelmaranon@hotmail.es maria-teresa.rivas@unirioja.es

July 2, 2013

Abstract

In this work, we develop and implement two algorithms for plotting and computing the measure of the basins of attraction of rational maps defined on the Riemann sphere. These algorithms are based on the subdivisions of a cubical decomposition of a sphere and they have been made by using different computational environments.

As an application, we study the basins of attraction of the fixed points of the rational functions obtained when Newton's method is applied to a polynomial with two roots of multiplicities m and n . We focus our attention on the analysis of the influence of the multiplicities m and n on the measure of the two basins of attraction. As a consequence of the numerical results given in this work, we conclude that, if $m > n$, the probability that a point in the Riemann Sphere belongs to the basin of the root with multiplicity m is bigger than the other case. In addition, if n is fixed and m tends to infinity, the probability of reaching the root with multiplicity n tends to zero.

*2010 MATHEMATICS SUBJECT CLASSIFICATION: 65H04, 65Y99, 54H20.

†KEY WORDS AND PHRASES: NEWTON'S METHOD, BASIN OF ATTRACTION, MULTIPLICITY OF A ROOT, SUBDIVISIONS ON THE SPHERE, MEASURE ALGORITHMS.

‡The authors acknowledge the financial help given by the projects: MTM2011-28636-C02-01 of the Spanish Ministry of Science and Technology and API12/10 of the University of La Rioja.

1 Introduction

Let $p : \mathbb{C} \rightarrow \mathbb{C}$ be a d -degree polynomial whose roots are not necessarily distinct and let N_p be the iterating function of the well-known Newton's method:

$$z_{n+1} = N_p(z_n) = z_n - \frac{p(z_n)}{p'(z_n)}. \quad (1)$$

It is well-known, [2], [9], that if the previous sequence starts at an initial approximation, z_0 , close enough to a root of the polynomial p , then it converges to such root. If the root is simple, the order of convergence of the sequence (1) is quadratic but if the root is multiple, the order of convergence is only linear. This fact reveals that the multiplicity of the roots plays an important role in the convergence of Newton's method.

There are other effects of the multiplicity of the roots in Newton's method. For instance, when Newton's method is applied to d -degree polynomials with simple roots, a rational function of degree d is obtained. However, for multiple roots the degree of the corresponding rational function is strictly less than d .

The classical Cayley's problem [8] is related to the basins of attraction of the roots of a quadratic polynomial when Newton's method is considered. To be more precise, Newton's method is applied to the polynomial $p(z) = (z - \alpha_1)(z - \alpha_2)$, where α_1 and α_2 are two distinct complex roots. Let us denote

$$\text{Basin}(\alpha_i) = \{z_0 \in \mathbb{C} : N_p^k(z_0) \rightarrow \alpha_i, k \rightarrow +\infty\}, \quad i = 1, 2$$

to the i -th basin of attraction ($N_p^k = N_p \circ \dots \circ N_p$, k -times). Cayley was able to show that, if $|z_0 - \alpha_1| < |z_0 - \alpha_2|$, then $z_0 \in \text{Basin}(\alpha_1)$ and that $z_0 \in \text{Basin}(\alpha_2)$ if $|z_0 - \alpha_2| < |z_0 - \alpha_1|$. The Julia set related to this problem ([3] for more details) is the frontier of both basins of attraction, that is, the Julia set for Newton's method (1) applied to the quadratic polynomial $p(z) = (z - \alpha_1)(z - \alpha_2)$ is the locus of points equidistant from the two roots. This problem has been profusely studied in the mathematical literature, not only for Newton's method but also for other different iterative procedures for solving nonlinear equations [1]. Furthermore, when Newton's method is applied to polynomials in the form $p(z) = (z - \alpha_1)^m(z - \alpha_2)^m$, with $m \geq 1$, it is also known, [17], that the Julia set is again the perpendicular bisector of the segment joining the roots α_1 and α_2 . That is, when the roots have the same multiplicity, the Julia set is a line. However, when the roots α_1 and α_2 have different multiplicity, the structure of the Julia set is more intricate. This fact was pointed out by Gilbert in [5] for the cubic polynomial $p(z) = (z - \alpha_1)^2(z - \alpha_2)$. The sensitivity of Julia sets to the multiplicity of the roots was also analyzed by Wang Xingyuan et al. (see [12] or [13], for instance). In these papers we can find that there are many other factors that could have an influence on the structure of the Julia set related with Newton's method applied to polynomials, such as the symmetries between the roots.

In this paper, we go a step beyond and analyze the influence of the multiplicities of the roots in the corresponding basins of attraction when Newton's

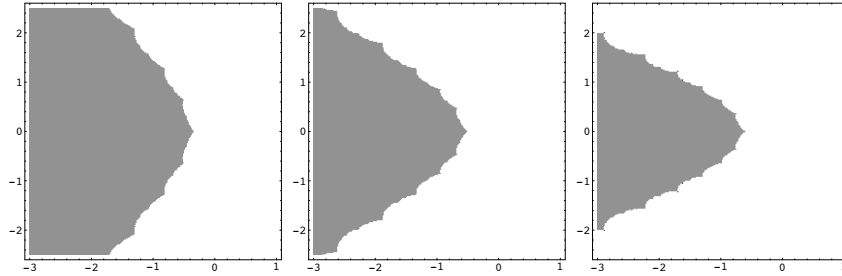


Figure 1: Basins of attraction of Newton’s method applied to the polynomials $p(z) = (z - 1)^m(z + 1)$ for $m = 2, 3, 4$. We see how the basin of the multiple root (in white) “invades” the other basin (in grey) when m increases.

method (1) is applied to polynomials in the form:

$$p(z) = (z - \alpha_1)^m(z - \alpha_2)^n, \alpha_1, \alpha_2 \in \mathbb{C}, \alpha_1 \neq \alpha_2, m, n \in \mathbb{N} \setminus \{0\}. \quad (2)$$

For each polynomial $p(z)$ in (2), the application of Newton’s method (1) gives a rational function, $B_{m,n}(z)$, whose coefficients depend on the multiplicities m, n :

$$B_{m,n}(z) = \frac{-\alpha_1\alpha_2 + \alpha_1z + \alpha_2z - \alpha_2mz - \alpha_1nz - z^2 + mz^2 + nz^2}{-\alpha_2m - \alpha_1n + mz + nz}. \quad (3)$$

Notice that the rational function $B_{m,n}(z)$ has quadratic degree, regardless of the values of the multiplicities m and n .

In our work, we are interested in the study of the influence of the multiplicity on the geometrical properties of the basins (and Julia sets) associated with the rational function $B_{m,n}(z)$. This implies that we can only modify the rational functions of this type using transformations preserving the geometrical properties of the basins that we are studying.

As a starting point in our study, we consider the roots $\alpha_1 = 1, \alpha_2 = -1$. A first graphical inspection (see Figure 1) shows that there exists a clear influence of the multiplicities of the roots on the shapes of the basins of attraction.

We can also observe that the basin of the root with higher multiplicity invades the basin of the root with lower multiplicity. In Figure 1 we have considered the rectangle $[-3, 1] \times [-2.5, 2.5]$ as a framework. Then, in these rectangles one can see that the area of the corresponding basin (in white) of the root $z = 1$ increases when the multiplicity m increases ($m = 2, 3, 4$). Since it is known that the areas of the complete basins in the complex plane \mathbb{C} is not finite, this property cannot be easily extended to compare the complete basins. However, this difficulty can be avoided using the canonical bijection between the extended complex plane and the unit sphere $\mathbb{C} \cup \{\infty\} \cong S^2$. Using the usual measure of S^2 , we can calculate a new measure of the area of the basins in S^2 , with the important property that now these areas are finite. In this way we can compare the area of different complete basins.

Since the structure of the boundary of an attraction basin (the Julia set) is, in general, very complicated, the standard methods based on a good election of coordinates and integration theory using a volume (area) form cannot be easily applied. We have sorted out this problem by developing some combinatorial methods and using the excess of a spherical triangle to compute, module a given precision, the area of a basin in the Riemann sphere.

The main objective of this paper is to give a computational study of the influence of the multiplicity of the roots on the area of the attraction basins. Our study has been divided in three phases:

- (i) We have given two different computational algorithms to calculate the area of the basin of attraction of a fixed point of a rational function on the Riemann sphere. In addition, we have implemented one of them using *Sage* and the other one using *Mathematica*.
- (ii) We have applied these algorithms and their implementations to compute the area of the basins of attraction of the rational functions obtained when Newton's method is applied to a polynomial.
- (iii) In particular, for the case of a polynomial with two roots $p(z) = (z - 1)^m(z + 1)^n$, we have quantified the influence of the multiplicities m, n on the measure of the corresponding basins.

With this aim, the paper is organized as follows. Section 2 is devoted to recall some basic notions: discrete semi-flow, basin of attraction and canonical bijections between the Alexandroff compactification of \mathbb{C} , the 2-sphere and the complex projective line. The geometrical notions given in Section 3 allow us to introduce the usual measure on the 2-sphere in a computational way, by using consecutive subdivisions of a cubical structure on the 2-sphere and the Girard's theorem that gives the area of a spherical triangle in terms of the measure of its angles. The unit sphere is inscribed in the boundary of the 3-cube $[-1, 1]^3$ and the central projection gives a homeomorphism from the boundary of the 3-cube to the unit sphere. In our study, two canonical ways of subdivision are used: the projection of subdivisions of the boundary of the 3-cube or the subdivisions of the projection of the cube. Both of them induce the same standard measure on the unit 2-sphere; however, the second procedure gives a more homogeneous distribution of areas and, as a consequence, a faster algorithm, since fewer subdivisions are needed to achieve a given precision.

In Section 4, we give a description of the algorithms that we use to compute the measure of the area of the attraction basins of a rational map on the Riemann sphere. In addition, some implementation of these algorithms using the computer programs *Mathematica* and *Sage* are described in Section 4.3. It is interesting to remark that the order of convergence plays an important role in the design of our algorithm, as we show in Subsection 4.1.2. To avoid some problems derived from the slow convergence in case of linear order of convergence, we have worked with two different precisions: 10^{-c_1} and 10^{-c_2} . In the case of Newton's

method, both precisions can be related with the formula $c_2 = c_1 - \log_{10}(m - 1)$, where m is the maximum of the multiplicities of the roots.

Finally, in Section 5 we study the effects of the multiplicity of the roots on the attraction basins of Newton's method applied to polynomials with two roots. In particular, we look for an answer to the following question: if we choose randomly a point in the Riemann sphere and we iterate the rational function given by Newton's method, what is the probability of the generated sequence to converge to a given root? So, we can associate to each root a probability with the above criterium. In the case of polynomials with two simple roots (Cayley's problem), it is clear that both roots have the same probability. However, the inspection of Figure 1 reveals that the probability related to the root with the biggest multiplicity is bigger than the other one. Although they could be many other ways to associate a probability to a root, in this paper we have used the area (divided by the area of the sphere) of the corresponding basin of attraction in the Riemann sphere as the probability of the root. Section 5 contains also some numerical experiments with values of the probabilities of the fixed points 1 and -1 of the rational function $B_{m,n}$ introduced in (3) as a function of m and n , or more generally, probabilities of polynomials with two unitary opposite roots $\alpha_1 = -\alpha_2$ ($|\alpha_1| = |\alpha_2| = 1$). In section 6, some future applications and research lines are analyzed.

2 Mathematical framework

In order to create a theoretical basis to hold and justify the correct construction of our algorithms for the representation of basins of end points of rational maps, we shall use the mathematical techniques described in this section. This study will be developed within the theoretical framework of complex dynamics on the Riemann sphere.

2.1 Discrete semi-flows and basins

A discrete semi-flow on a (topological space) set X is a (continuous) map $\varphi: \mathbb{N} \times X \rightarrow X$ such that $\varphi(0, p) = p$, $\forall p \in X$ and $\varphi(n, \varphi(m, p)) = \varphi(n+m, p)$, $\forall p \in X$, $\forall n, m \in \mathbb{N}$. We shall use $n \cdot x = \varphi(n, x)$ for short.

Given a discrete semi-flow $\varphi: \mathbb{N} \times X \rightarrow X$, $n_0 \in \mathbb{N}$, $x_0 \in X$, we have the induced maps $\varphi^{n_0}: X \rightarrow X$, $\varphi^{n_0}(x) = \varphi(n_0, x)$, and the orbit of x_0 given by $\varphi_{x_0}: \mathbb{N} \rightarrow X$, $\varphi_{x_0}(n) = \varphi(n, x_0)$. Note that a discrete semi-flow $\varphi: \mathbb{N} \times X \rightarrow X$ induces a map $\varphi^1: X \rightarrow X$ and, conversely, a (continuous) map $f: X \rightarrow X$ induces a discrete semi-flow $\varphi: \mathbb{N} \times X \rightarrow X$ given by $\varphi(n, x) = f^n(x)$, where f^n denotes the function composition $f \circ \dots \circ f$ and $f^0 = \text{Id}_X$. The discrete semi-flow induced by f will be denoted by (X, f) or X for short.

Let X be a discrete semi-flow. A point $x \in X$ is said to be a fixed point if, for all $n \in \mathbb{N}$, $n \cdot x = x$ and x is said to be a periodic point if there exists $n \in \mathbb{N}$, $n \neq 0$, such that $n \cdot x = x$.

Let (X, d) be a metric space with metric d . Given a discrete semi-flow induced by a continuous map $f: X \rightarrow X$, the triplet (X, d, f) will be called metric discrete semi-flow. Next, we introduce a notion of end point based on the existence of the metric d ; for other notions of end point of a dynamical system, we refer the reader to [4].

Given a metric discrete semi-flow $X = (X, d, f)$, the *end point space* of X is defined as the quotient set

$$\Pi(X) = \frac{\{(f^n(x))_{n \in \mathbb{N}} \mid x \in X\}}{\sim},$$

where, given $x, y \in X$, $(f^n(x)) \sim (f^n(y))$ if and only if

$$(d(f^n(x), f^n(y))) \xrightarrow{n \rightarrow +\infty} 0.$$

An element $a = [(f^n(x))] \in \Pi(X)$ is called an *end point* of the metric discrete semi-flow.

Notice that one can define a natural map

$$\omega: X \rightarrow \Pi(X)$$

given by $\omega(x) = [(f^n(x))] = [(x, f(x), f^2(x), \dots)]$. The subset denoted by

$$\text{Basin}(a) = \omega^{-1}(a), \quad a \in \Pi(X)$$

is called the *basin of the end point* a .

The map ω allows us to decompose any metric discrete semi-flow as follows:

$$X = \bigsqcup_{a \in \Pi(X, d)} \text{Basin}(a).$$

This decomposition will be called the ω -*decomposition* of the metric discrete semi-flow X .

Note that a fixed point y can be interpreted as an end point $[(y)] = [(y, y, \dots)] \in \Pi(X)$ and, in this case, one obtains the notion of attraction basin given in the introduction.

2.2 Basins of rational functions on the Riemann sphere

Let $S^2 = \{(r_1, r_2, r_3) \in \mathbb{R}^3 \mid r_1^2 + r_2^2 + r_3^2 = 1\}$ be the unit 2-sphere and let $N = (0, 0, 1)$ be the north pole.

We can consider in a natural way a bijection $\tilde{\theta}: S^2 \rightarrow \mathbb{C} \cup \{\infty\}$ given as follows:

$$\tilde{\theta}(r_1, r_2, r_3) = \begin{cases} \frac{r_1}{1-r_3} + i \frac{r_2}{1-r_3}, & \text{if } r_3 < 1, \\ \infty, & \text{if } r_3 = 1. \end{cases}$$

Besides, we can take the equivalence relation on $\mathbb{C}^2 \setminus \{(0, 0)\}$: $(z, t) \sim (z', t')$ if there exists $\lambda \in \mathbb{C} \setminus \{0\}$ such that $(z, t) = (\lambda z', \lambda t')$. The equivalence class

of (z, t) is denoted by $[z, t]$ and the quotient set is denoted by $\mathbf{P}^1(\mathbb{C})$ and it is called the complex projective line.

Given a point $[z, t] \in \mathbf{P}^1(\mathbb{C})$, the coordinates (z, t) are called the homogeneous coordinates of the point and t/z (or z/t where appropriate) are the absolute coordinates of that point. In our study, we often use normalized homogeneous coordinates for any point in $\mathbf{P}^1(\mathbb{C})$, which are given as follows:

$$[z, t] = \begin{cases} [z/t, 1], & \text{if } |t| \geq |z|, \\ [1, t/z], & \text{if } |t| < |z|, \end{cases}$$

where $|t|$ and $|z|$ represent the absolute value (or modulus) of the complex numbers t and z , respectively.

We also have the induced bijection $\theta: \mathbf{P}^1(\mathbb{C}) \rightarrow \mathbb{C} \cup \{\infty\}$ given by

$$\theta([z, t]) = \begin{cases} z/t, & \text{if } t \neq 0, \\ \infty, & \text{if } t = 0. \end{cases}$$

The pair of bijections above induce a new bijection $\theta^{-1}\tilde{\theta}: S^2 \rightarrow \mathbf{P}^1(\mathbb{C})$, which is defined as follows:

$$\theta^{-1}\tilde{\theta}(r_1, r_2, r_3) = [r_1 + ir_2, 1 - r_3].$$

The inverse map of this bijection $\tilde{\theta}^{-1}\theta: \mathbf{P}^1(\mathbb{C}) \rightarrow S^2$ is given by the following formula:

$$\tilde{\theta}^{-1}\theta([z, t]) = \left(\frac{\bar{z}t + z\bar{t}}{tt + z\bar{z}}, \frac{i(\bar{z}t - z\bar{t})}{tt + z\bar{z}}, \frac{-\bar{t}t + z\bar{z}}{tt + z\bar{z}} \right).$$

We recall that a surface with a 1-dimensional complex structure is said to be a Riemann surface and a Riemann surface of genus 0 is said to be a Riemann sphere. Using the bijections defined above, we have that S^2 and $\mathbb{C} \cup \{\infty\}$ are Riemann spheres.

Let $h: \mathbb{C} \rightarrow \mathbb{C}$ be a rational function in the form $h(u) = a \frac{F(u)}{G(u)}$, where $u, a \in \mathbb{C}$, $a \neq 0$, $F(u) = (u - z_1) \cdots (u - z_p) = u^p + a_1 u^{p-1} + \cdots + a_p$ and $G(u) = (u - l_1) \cdots (u - l_q) = u^q + b_1 u^{q-1} + \cdots + b_q$. Suppose that $\{z_1, \dots, z_p\} \cap \{l_1, \dots, l_q\} = \emptyset$. Then, the function h induces an extension map $h^+: \mathbb{C} \cup \{\infty\} \rightarrow \mathbb{C} \cup \{\infty\}$, where $h^+(l_i) = \infty$ and $h^+(\infty) \in \{\infty, 0, a\}$ and its value depends on the degrees of F and G .

It is important to notice that, in the case that we take $u = z/t$ and $d = \max\{p, q\}$ in the expression

$$\frac{a(u^p + a_1 u^{p-1} + \cdots + a_p)}{(u^q + b_1 u^{q-1} + \cdots + b_q)},$$

we have

$$\frac{a(z^p t^{d-p} + a_1 z^{p-1} t^{d-p+1} + \cdots + a_p t^d)}{z^q t^{d-q} + b_1 z^{q-1} t^{d-q+1} + \cdots + b_q t^d}.$$

Then, we obtain the following homogeneous polynomials of degree d in the variables z, t :

$$\begin{aligned} A(z, t) &= a(z^p t^{d-p} + a_1 z^{p-1} t^{d-p+1} + \dots + a_p t^d), \\ B(z, t) &= z^q t^{d-q} + b_1 z^{q-1} t^{d-q+1} + \dots + b_q t^d. \end{aligned}$$

The bijection $\theta: \mathbf{P}^1(\mathbb{C}) \rightarrow \mathbb{C} \cup \{\infty\}$ induces the map $h^1: \mathbf{P}^1(\mathbb{C}) \rightarrow \mathbf{P}^1(\mathbb{C})$ defined by $h^1 = \theta^{-1} h^+ \theta$, which is expressed in homogeneous coordinates as follows:

$$h^1([z, t]) = [A(z, t), B(z, t)].$$

We can see that if f is a rational map represented by a pair of coprime homogeneous polynomials $A(z, t), B(z, t)$ of degree d , then the set $\{[z_1, t_1], \dots, [z_{n+1}, t_{n+1}]\}$ of roots of $A(z, t)t - B(z, t)z$ is the set of fixed points of f and the iterated map f^r is a rational map of degree d^r which has $d^r + 1$ fixed points (taking into account its multiplicity).

Remark 1. *The representation of a rational function with a pair of homogeneous polynomials in two variables with the same degree combined with normalized homogeneous coordinates permits to work with poles and the point at infinity, as well as to avoid overflows and underflows in our algorithms.*

We also recall that one has two natural metrics on S^2 : since S^2 is a subspace of \mathbb{R}^3 , the usual Euclidean metric of \mathbb{R}^3 induces an Euclidean metric d^E on S^2 , which is called chordal metric; besides, we have as well that S^2 inheres a Riemannian metric d^R from the canonical Riemannian structure of $S^2 \subset \mathbb{R}^3$. The connection between the Riemannian metric d^R and the Euclidean metric d^E on S^2 is given by the expression:

$$d^E((r_1, r_2, r_3), (r'_1, r'_2, r'_3)) = 2 \sin \left(\frac{d^R((r_1, r_2, r_3), (r'_1, r'_2, r'_3))}{2} \right).$$

Using the bijection $\tilde{\theta}^{-1}\theta: \mathbf{P}^1(\mathbb{C}) \rightarrow S^2$, we can translate the metric structures from S^2 to $\mathbf{P}^1(\mathbb{C})$ with the following formulas:

$$\begin{aligned} d_1^E([z, t], [z', t']) &= d^E(\tilde{\theta}^{-1}\theta([z, t]), \tilde{\theta}^{-1}\theta([z', t'])), \\ d_1^R([z, t], [z', t']) &= d^R(\tilde{\theta}^{-1}\theta([z, t]), \tilde{\theta}^{-1}\theta([z', t'])). \end{aligned}$$

An explicit formula for the chordal metric d_1^E is given by:

$$d_1^E([z, t], [z', t']) = \left(\left(\frac{\bar{z}t + z\bar{t}}{t\bar{t} + z\bar{z}} - \frac{\bar{z}'t' + z'\bar{t}'}{t't' + z'\bar{z}'} \right)^2 + \left(\frac{i(\bar{z}t - z\bar{t})}{t\bar{t} + z\bar{z}} - \frac{i(\bar{z}'t' - z'\bar{t}')}{t't' + z'\bar{z}'} \right)^2 + \left(\frac{-t\bar{t} + z\bar{z}}{t\bar{t} + z\bar{z}} - \frac{-t'\bar{t}' + z'\bar{z}'}{t't' + z'\bar{z}'} \right)^2 \right)^{\frac{1}{2}}.$$

In this paper, we consider the metric space (X, d, f) , where $X = S^2 \cong \mathbb{C} \cup \{\infty\} \cong \mathbf{P}^1(\mathbb{C})$, $d = d^E$ is the chordal metric on S^2 and f is a rational map.

The canonical map

$$\omega: S^2 \rightarrow \Pi(S^2, d^E)$$

given by $\omega(x) = [(x, f(x), f^2(x), \dots)]$ decomposes the 2-sphere as a disjoint union of basins of end points. One of the objectives of this paper is to develop some algorithms to compute the area of these basins.

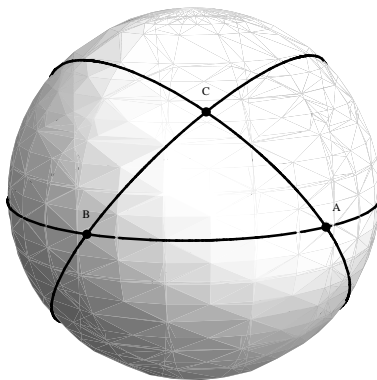


Figure 2: An example of a spherical triangle.

3 Cubic subdivisions of the sphere and measure functions

In this section, we describe a computational method to give a measure function on a sphere based on the excess of a spherical quadrilateral and a system of consecutive subdivisions of the sphere.

A spherical triangle ABC is formed by connecting three points on the surface of a sphere with great arcs, so that these three points do not lie on a great circle of the sphere (see Figure 2). The angle at each vertex is measured as the angle between the tangents to the incident sides in the vertex tangent plane.

Theorem 1. *Let ABC be a triangle on a sphere of radius R with each angle smaller than π . Then, the area of the spherical triangle ABC is*

$$\mu(ABC) = (\angle A + \angle B + \angle C - \pi)R^2.$$

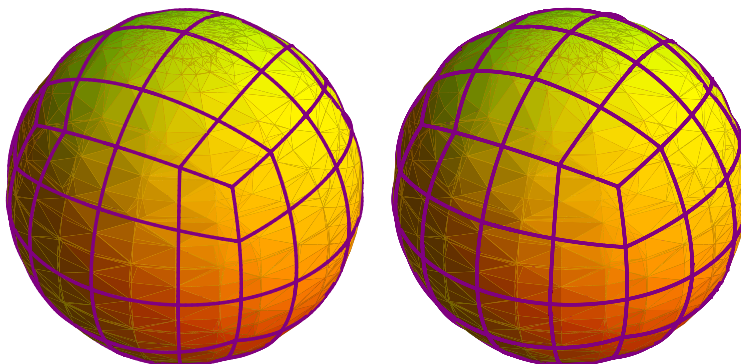
The condition that each angle of the triangle is smaller than π avoids a possible ambiguity between the triangle or its complement on the sphere. This result is also known as Girard's theorem and the value $(\angle A + \angle B + \angle C - \pi)$ is called the *excess* of the spherical triangle. We recall that a similar formula is used in the hyperbolic plane to give the area of a triangle, but in this case one has to take the defect $\pi - (\angle A + \angle B + \angle C)$.

A spherical quadrilateral $ABCD$ is defined in a similar way. As a consequence of Girard's theorem, one obtains:

Corollary 1. *The area of a spherical quadrilateral $ABCD$ on a sphere of radius R is*

$$\mu(ABCD) = (\angle A + \angle B + \angle C + \angle D - 2\pi)R^2.$$

It is interesting to remark that in the case $R = 1$, one has that the area of a spherical triangle coincides with its excess and similarly for spherical quadrilaterals.



(a) The subdivision $\eta(\text{Sd}^2(\mathcal{S}))$.

(b) The subdivision $\text{Sd}^2(\eta(\mathcal{S}))$.

Figure 3: Processes of consecutive cubical subdivisions of the sphere.

3.1 Two different processes of consecutive subdivisions of the sphere

We note that the unit 2-sphere is inscribed in the boundary of the cube $[-1, 1]^3$ and the Euclidean norm induces a canonical projection

$$\eta: \partial([-1, 1]^3) \rightarrow S^2, \quad \eta(x) = \frac{x}{\|x\|}.$$

It is interesting to note that one has a canonical cubic structure \mathcal{S} of the boundary of the 3-cube (8 vertexes, 12 edges and 6 faces). Taking the barycenters of the cubes of \mathcal{S} , one can construct the canonical barycentric subdivision $\text{Sd}(\mathcal{S})$ and, for $r = 0, 1, 2, \dots$, we can apply consecutively the operator Sd to obtain the subdivisions $\text{Sd}^r(\mathcal{S})$.

The subdivision structures given above are transformed by η into new subdivisions of the 2-sphere:

$$\eta(\text{Sd}^r(\mathcal{S})).$$

For instance, for $r = 2$ one has the cubical structure of Figure 3(a).

We can follow a different strategy to obtain other type of consecutive cubical subdivisions of the sphere. To do this, we can use the following basic properties of the spherical geometry:

- (i) Given two non-antipodal points $A, B \in S^2$, ($A \neq B$), there is a unique spherical arc AB determined by A and B .
- (ii) Given a spherical arc AB , there is a unique middle point

$$(\widehat{AB}) = \frac{A + B}{\|A + B\|}.$$

(iii) Given a spherical quadrilateral $ABCD$, there is a unique middle point

$$(\widehat{ABCD}) = \frac{A + B + C + D}{\|A + B + C + D\|}.$$

(iv) A given spherical quadrilateral $ABCD$ admits a canonical subdivision given by the four spherical quadrilaterals:

$$\begin{aligned} A(\widehat{AB})(\widehat{ABCD})(\widehat{DA}), & \quad (\widehat{AB})B(\widehat{BC})(\widehat{ABCD}), \\ (\widehat{ABCD})(\widehat{BC})C(\widehat{CD}), & \quad (\widehat{CD})D(\widehat{DA})(\widehat{ABCD}). \end{aligned}$$

In this way, we can subdivide each quadrilateral of $\eta(\mathcal{S})$ to obtain the subdivision $\text{Sd}(\eta(\mathcal{S}))$. Applying consecutively the operator Sd , for $r = 0, 1, 2, \dots$, one has the r -th subdivision:

$$\text{Sd}^r(\eta(\mathcal{S})),$$

which can be seen for $r = 2$ in Figure 3(b).

Remark 2. *It is interesting to observe that we have described two different processes to obtain consecutive cubical subdivisions of the 2-sphere: $\eta(\text{Sd}^r(\mathcal{S}))$ and $\text{Sd}^r(\eta(\mathcal{S}))$. In order to compute the measure of a basin, the authors have developed algorithms implemented in Sage to construct the subdivisions $\eta(\text{Sd}^r(\mathcal{S}))$ and other algorithms implemented in Mathematica to construct $\text{Sd}^r(\eta(\mathcal{S}))$. This will permit us to compare different algorithms and different computational environments.*

3.2 Measures and probabilities induced by consecutive subdivisions

A sequence of consecutive subdivisions Γ^r of the 2-sphere permits us to consider the 2-sphere as a measure space and, dividing the measure function by the area of the 2-sphere, one obtains a canonical structure of probability space. In order to calculate the area of a spherical quadrilateral $ABCD$ of a given subdivision, it suffices to apply the formula given in Corollary 1:

$$\mu(ABCD) = \angle A + \angle B + \angle C + \angle D - 2\pi.$$

Denote by $\text{Sd}(ABCD)$ the family of the new spherical quadrilaterals of a subdivision of a spherical quadrilateral $ABCD$ and by $\mu(\text{Sd}(ABCD))$ the sum of the areas of the quadrilaterals of the subdivision of $ABCD$ using the formula above. Taking into account that the sum of the measures of the angles at some vertexes is π or 2π , it is easy to check that

$$\mu(\text{Sd}(ABCD)) = \mu(ABCD).$$

To extend this measure procedure to a more general subset A of the unit 2-sphere, we suppose that the subdivision sequence satisfies the following condition: if σ_r is a quadrilateral of Γ^r , then $\lim_{r \rightarrow +\infty} (\mu(\sigma_r)) = 0$.

Now, the family of measurable subsets can be introduced as follows. Let $A \subset S^2$ and consider the following families of spherical quadrilaterals and areas:

$$S(A, r) = \{\sigma \in \Gamma^r \mid A \cap \sigma \neq \emptyset\}, \quad S_A^r = \sum_{\sigma \in S(A, r)} \mu(\sigma)$$

and

$$s(A, r) = \{\sigma \in \Gamma^r \mid \sigma \subset A\}, \quad s_A^r = \sum_{\sigma \in s(A, r)} \mu(\sigma),$$

where, in case that $s(A, r)$ is empty, one takes $s_A^r = 0$.

So, as a consequence of the following result, one has an increasing sequence of lower sums s_A^r and a decreasing sequence of upper sums S_A^r .

Lemma 1. *Let $A \subset S^2$ and suppose that Γ^{r+1} is a subdivision of Γ^r . Then,*

- (i) $s(A, r) \subset S(A, r), \quad s_A^r \leq S_A^r;$
- (ii) $\text{Sd}(s(A, r)) \subset s(A, r+1) \subset S(A, r+1) \subset \text{Sd}(S(A, r)),$
 $\mu(\text{Sd}(s(A, r))) = s_A^r, \mu(\text{Sd}(S(A, r))) = S_A^r;$
- (iii) $s_A^r \leq s_A^{r+1} \leq S_A^{r+1} \leq S_A^r.$

Definition 1. *Let A be a subset of the unit sphere S^2 . The limit $s_A = \lim_{r \rightarrow +\infty} s_A^r$ is said to be the lower sum of A and $S_A = \lim_{r \rightarrow +\infty} S_A^r$ is said to be the upper sum of A . $A \subseteq S^2$ is said to be measurable if $s_A = S_A$, and $s = s_A = S_A$ is said to be the measure or area of A . The probability measure of A is given by $P(A) = s/4\pi$.*

Remark 3. *The measure μ can be also considered as a solid angle measure which generalizes to dimension 2 the usual circle angle measure.*

The measure in the 2-sphere can be also introduced using a volume form, and the measure of many regions whose boundary is given by a smooth curve can be computed in many cases using suitable coordinates and by usual integration formulas. However, many problems appear when one wants to compute the area of an attraction basin whose frontier is a Julia set whose fractal dimension is between 1 and 2 and its length (if the Julia set can be considered as a measurable set) could be infinite.

In this paper, we describe some computational algorithms to give the area or probability of the basin of a fixed point of a rational function on the Riemann sphere. As an application, we compute, up to a given precision, the area of attraction basins of the rational function obtained by applying Newton's method to a polynomial and we also quantify the influence of the multiplicity for the case of a polynomial with two roots.

4 Multiplicity, algorithms and implementations

In the previous sections, we have introduced some mathematical techniques and developed basic theoretical aspects necessary to build computer programs with the ability of representing attraction basins of end points associated to a determined rational function. We shall show in the next lines the algorithms which have been developed to study the basins induced by a rational function f on the Riemann 2-sphere.

4.1 Influence of the multiplicity on the design of algorithms

The authors (see Ref. [7]) have developed some algorithms and implementations to plot the different basins of a rational map. However, when the order of convergence is linear, the modifications described below are convenient in order to obtain right plots and measure of basins.

4.1.1 Order of convergence bigger than one

With a view to find an end point associated to a point $x \in S^2$, the rational map f must be iterated to obtain a finite sequence

$$(x, f(x), f^2(x), f^3(x), \dots, f^{k-1}(x), f^k(x)).$$

In this context, a maximum number of iterations l must be considered and a certain precision c must be prefixed to determine when to stop the iterative process while programming the function which returns such sequence. That is why we shall always work with sequences in which $k \leq l$.

After each iteration, there will be two possible cases:

- 1) If the chordal distance from $f^{k-1}(x)$ to $f^k(x)$ is lower than 10^{-c} , then the list $[f^k(x), k]$ is taken as output; otherwise, case 2) is applied.
- 2) If $k < l$, a new iteration is done and case 1) is applied again; otherwise (if $k = l$), then the output $[f^l(x), l]$ is taken.

Consider the ordered sequence of all fixed points $\{x_1, x_2, \dots, x_{h+1}\}$ associated to the rational map f . If m_1, m_2, \dots, m_{h+1} are the multiplicities of the fixed points, one has that $m_1 + m_2 + \dots + m_{h+1} = d + 1$, where d is the degree of the rational map.

Now, given a point $x \in S^2$, if we consider the iteration sequence $(x, f(x), f^2(x), f^3(x), \dots, f^{k-1}(x), f^k(x))$ and the corresponding output $[f^k(x), k]$ given by the sub-algorithm above, we have two cases: if there exists $i \in \{1, \dots, h+1\}$ such that the chordal distance from $f^k(x)$ to the fixed point x_i is lower than 10^{-c} , then the new sub-algorithm returns $[i, k]$; otherwise, one has $k = l$ and the output is taken to be $[0, l]$, where l is the maximum number of iterations which was prefixed beforehand.

Denote by $D_{x_i}^{c,l}$ the set of points for which the sub-algorithm returns $[i, k]$ ($k \leq l$) and denote $D^{c,l} = D_{x_1}^{c,l} \cup \dots \cup D_{x_{h+1}}^{c,l}$. We observe that $D_{x_i}^{c,l}$ is an approximation of the basin $\text{Basin}(x_i) = \omega^{-1}([x_i, x_i, \dots])$. In general, for a greater l and a greater c , one obtains better approximations of the attraction basins.

In this way, we have a decomposition of the Riemann 2-sphere:

$$S^2 = (S^2 \setminus D^{c,l}) \cup D_{x_1}^{c,l} \cup \dots \cup D_{x_{n+1}}^{c,l}.$$

It is interesting to observe that, when one has convergence of order greater than 1, then for large k the distance from $f^k(x)$ to the limit point is lower than the distance from $f^{k-1}(x)$ to $f^k(x)$. This fact cannot be true if a linear order of convergence is attained and, in that case, it is necessary a modification of the algorithm which is described in next subsection. This situation appears when we apply Newton's method to a polynomial with non-simple roots.

4.1.2 Modification of the algorithms in case of linear convergence

Suppose that we are working with a rational function f of the Riemann sphere and we are using the chordal distance $d = d^E$. If for a given point x one has that $f^k(x)$ converges to a given fixed point y and

$$\lim \left(\frac{d(f^{(k)}(x), y)}{d(f^{(k-1)}(x), y)} \right) = \lambda < 1,$$

then one has linear convergence.

The above algorithms have an important problem when the sequence $f^k(x)$ has linear convergence. In this case, for large k we have that

$$d(f^{(k)}(x), y) \sim \lambda d(f^{(k-1)}(x), y).$$

If we suppose that $d(f^k(x), y)$ is a decreasing sequence, then one has that

$$\begin{aligned} d(f^{(k)}(x), f^{(k-1)}(x)) &\geq d(f^{(k-1)}(x), y) - d(f^{(k)}(x), y) \\ &\sim \frac{1}{\lambda} d(f^{(k)}(x), y) - d(f^{(k)}(x), y) \\ &= \left(\frac{1}{\lambda} - 1 \right) d(f^{(k)}(x), y) \end{aligned}$$

or, equivalently, $d(f^{(k)}(x), y) \lesssim \frac{\lambda}{1-\lambda} d(f^{(k)}(x), f^{(k-1)}(y))$.

For Newton's method, if we consider the rational map $f = N_p$, where p is a polynomial, one of the difficulties with the numerical calculation of a multiple root of multiplicity m is that the convergence is slower than for the case of a simple root. For a root of multiplicity m , one has linear convergence with $\lambda = 1 - (1/m)$; hence, $\frac{\lambda}{1-\lambda} = m - 1$, and, therefore,

$$d(f^{(k)}(x), y) \lesssim (m - 1) d(f^{(k)}(x), f^{(k-1)}(y)).$$

Then, for a large k , in the case that $d(f^{(k)}(x), y) \sim (m-1)d(f^{(k)}(x), f^{(k-1)}(y))$, one could have that

$$d(f^{(k-1)}(x), y) \sim (m-1)d(f^{(k)}(x), f^{(k-1)}(y)).$$

This implies that, when the iterative process stops because

$$d(f^{(k)}(x), f^{(k-1)}(x)) \sim 10^{-c},$$

then one can have $d(f^{(k)}(x), y) \sim (m-1)10^{-c} > 10^{-c}$ ($m > 2$) and the algorithm will give a wrong result, which is that x is not in the basin of y .

This problem can be avoided working with two precision numbers: 10^{-c_1} is the precision we use in order to stop the iteration process and a new precision 10^{-c_2} can be introduced to determine if the final point of the iteration is close to a given root (fixed point) of multiplicity $m > 2$. In order to compare both precision numbers, as a consequence of the effect of multiplicity m , one has $10^{-c_2} \sim (m-1)10^{-c_1}$; thus, it suffices to take

$$c_2 = c_1 - \log_{10}(m-1).$$

In general, for a polynomial with at least one non-simple root and multiplicities m_1, \dots, m_s , one can take $c_2 = c_1 - \log_{10}(\max\{m_1 - 1, \dots, m_s - 1\})$ to compute the basins of the corresponding rational function and their measure.

4.2 Algorithms to compute the area of the basins of end points

4.2.1 Projection of subdivisions: $\eta(\text{Sd}^r(\mathcal{S}))$

For each 2-cube σ of $\text{Sd}^r(\mathcal{S})$, we compute its barycenter $\hat{\sigma}$ and the point $\eta(\hat{\sigma})$. After that, we use the algorithm given in the previous section to check whether $\eta(\hat{\sigma})$ is in the basin of one of the fixed points x_1, \dots, x_{h+1} (we remark that we have a prefixed maximal number of iterations l , as well as precisions 10^{-c_1} and 10^{-c_2}). We have two possibilities: if $\eta(\hat{\sigma})$ is in the basin of a fixed point x_i , then the 2-cube $\eta(\sigma)$ is included in a list of 2-cubes $L_i(r)$ associated with the fixed point x_i ; otherwise, the 2-cube σ is not included in any of the lists $L_1(r), \dots, L_{h+1}(r)$.

For each list $L_i(r)$, we can compute the finite sum of the areas of its spherical 2-cubes (quadrilaterals) $\mu(L_i(r)) = \sum_{\sigma \in L_i(r)} \mu(\eta(\sigma))$, where the area $\mu(\eta(\sigma))$ is given by computing the excess of the spherical quadrilateral $\eta(\sigma)$, see Corollary 1. In order to calculate the probability, it suffices to divide by the area 4π of the unit 2-sphere.

If you want to obtain the area module a precision 10^{-c} , you have to repeat the process above for higher values of r until you find one such that $|\mu(L_i(r)) - \mu(L_i(r+1))| < 10^{-c}$. Now, take $\mu(L_i(r+1))$ as the area of the basin of x_i .

Note the following fact: our algorithm states that, if the point $\eta(\hat{\sigma})$ is in the basin of a fixed point, then every point of $\eta(\sigma)$ is contained in the basin. Since

we can work with very fine subdivisions, this is not a big problem; however, this step of the algorithm can be improved checking that more points of $\eta(\sigma)$ are in the same basin or using more information, for example, the value of the derivative of an iterated function at $\eta(\hat{\sigma})$.

4.2.2 Subdivisions of the projection: $\text{Sd}^r(\eta(\mathcal{S}))$

In this case, the algorithm is similar to the process above. The difference is that we consider consecutive subdivisions of the first projection instead of projections of consecutive subdivisions, see subsection 3.1.

The main difference of this second process, $\text{Sd}^r(\eta(\mathcal{S}))$, is that the areas of the 2-cubes of a given subdivision are more similar than those of the 2-cubes obtained by $\eta(\text{Sd}^r(\mathcal{S}))$.

This implies that the election of “middle points” is more homogeneous in this second method than in the first method and, as a consequence, we can obtain a better approximation of the area of a basin for the same subdivision order. The fact that the distributions of areas is more homogeneous can be seen just by looking the following matrices M_1 and M_2 , which represent the areas of the “2-cubes” of the second subdivision of one of the six faces corresponding to the boundary of the cube $[-1, 1]^3$ by using respectively the first method, $\eta(\text{Sd}^2(\mathcal{S}))$, or the second one, $\text{Sd}^2(\eta(\mathcal{S}))$, illustrated in Figures 3(a), 3(b).

$$M_1 = \begin{pmatrix} 0.0814556 & 0.120393 & 0.120393 & 0.0814556 \\ 0.120393 & 0.201358 & 0.201358 & 0.120393 \\ 0.120393 & 0.201358 & 0.201358 & 0.120393 \\ 0.0814556 & 0.120393 & 0.120393 & 0.0814556 \end{pmatrix}$$

$$M_2 = \begin{pmatrix} 0.109805 & 0.131197 & 0.131197 & 0.109805 \\ 0.131197 & 0.151401 & 0.151401 & 0.131197 \\ 0.131197 & 0.151401 & 0.151401 & 0.131197 \\ 0.109805 & 0.131197 & 0.131197 & 0.109805 \end{pmatrix}$$

Note that the distribution of the areas is more homogeneous in the second matrix; that is, the discrepancy between the areas is lower in the second case than in the first one.

4.3 Implementation of graphic and probability algorithms in *Sage* and *Mathematica*

We have implemented in *Sage* the first algorithm (projection of subdivisions), **cubicProbabilityList**, to compute the probabilities of the different basins and we have constructed the function **cubicSpherePlot** to plot the attraction basins of a root (for other plotting programs on the plane, see also [10]). For more details about the implementation in *Sage*, we refer the reader to [7]. We have also implemented new versions working with two precisions c_1 , c_2 in order to avoid the possible problems originated when the order of convergence is lineal.

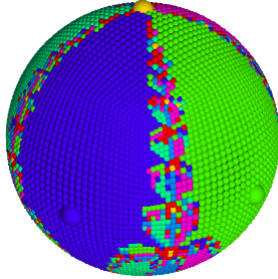


Figure 4: Plot of the attraction basins of the roots of the equation $z^5 - 1 = 0$ in the Riemann sphere.

Besides, we have also implemented the second algorithm (subdivisions of the projection) using *Mathematica*.

In next section, we shall see how these two different algorithms implemented in two different environments give similar results when one computes the measure of the basins of some rational function.

For example, the fractal showed in Figure 4 was plotted by applying the above *Sage* function `cubicSpherePlot` to the rational function

$$N_p = \frac{4x^5 + 1}{5x^4},$$

which is obtained when Newton's method is used to compute the roots of the equation $p(z) = z^5 - 1 = 0$.

5 Quantifying the influence of multiplicity with numerical experiments

In this section, we use the algorithms seen in the previous section to analyze the influence of the multiplicities m and n on the basins of attraction of the fixed points of a rational function in the form $B_{m,n}$ given in (3). In particular, for polynomials

$$p(z) = (z - 1)^m(z + 1)^n, \quad m, n \in \mathbb{N} \setminus \{0\}, \quad (4)$$

$B_{m,n}$ can be written as follows:

$$B_{m,n}(z) = \frac{(m + n - 1)z^2 + (m - n)z + 1}{(m + n)z + (m - n)}. \quad (5)$$

Subsequently, our experiment allow us to show the influence of the multiplicities on the probabilities related to the roots 1 and -1 of the polynomial (4), as

explained in Section 1. Taking into account the criterium which was introduced there, for each $m, n \in \mathbb{N}$ we denote by $P_1(m, n)$ the probability of the root $z = 1$ and by $P_{-1}(m, n)$ the probability of the root $z = -1$; that is,

$$P_{-1}(m, n) = \frac{A_{-1}}{4\pi}, \quad P_1(m, n) = \frac{A_1}{4\pi},$$

where A_{-1} and A_1 are respectively the areas of the basins of attraction in the Riemann sphere of the roots -1 and 1 , considered as fixed points of (5).

5.1 A graphic approach plotted with *Sage*

In Figure 5, we have plotted the basins of attraction of the roots $z = -1$ and $z = 1$ for different values of m and n ($m > n$). We can see how the basin of the root $z = -1$ is smaller than the other basin. In addition, we have quantified this graphical fact by calculating the probability related with the two roots. In fact, we only have included the values of $P_{-1}(m, n)$, because $P_1(m, n) = 1 - P_{-1}(m, n)$. In order to obtain these images, we have used the projection of a subdivision with order $r = 5$.

Our numerical experiments reveals the following facts:

- (i) It is necessary to increase the number of maximum iterations when multiplicities m and n go up.
- (ii) For a fixed m , the function $P_{-1}(m, n)$ is increasing on the variable n .
- (iii) For a fixed n , the function $P_{-1}(m, n)$ is decreasing on the variable m .
- (iv) For a fixed (m, n) , $m \geq n$, the function $P_{-1}(m + s, n + s)$ is increasing on the integer variable $s \geq 0$.

5.2 Computing the precision obtained using two consecutive subdivisions

In Table 1, we have gathered the values of probabilities $P_{-1}^{M^5}(m, n)$ for $1 \leq m \leq 8$ and $1 \leq n \leq 8$ when taking the fifth subdivision $\text{Sd}^5(\eta(\mathcal{S}))$ and a maximum number of iterations equal to 100. These probabilities have been calculated using the process described in paragraph 4.2.2 implemented in *Mathematica*.

Note that one has

$$P_{-1}(m, n) + P_{-1}(n, m) = 1.$$

From the results obtained by this simulation, one also obtains that the Julia set in S^2 has probability measure equal to zero and the same happens for the basins associated to periodic points, so that

$$P_{-1}(m, n) + P_1(m, n) = 1.$$

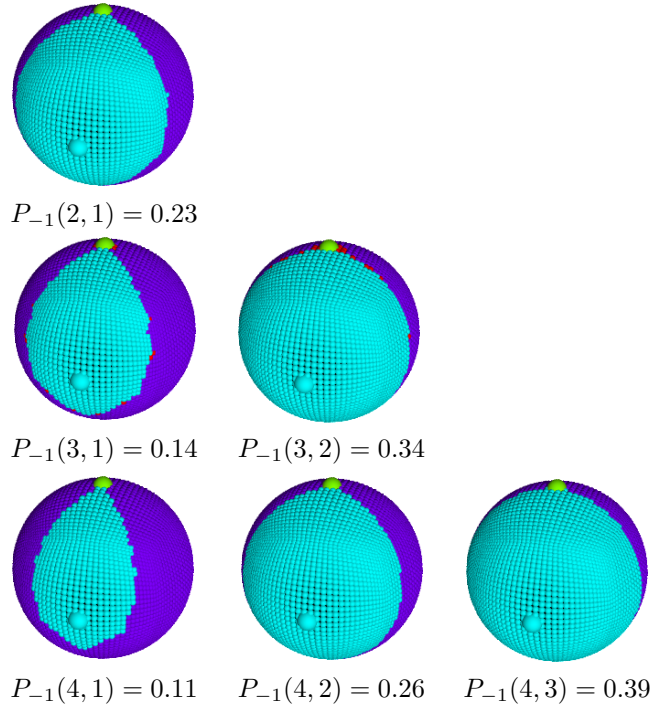


Figure 5: Basins on the Riemann sphere of the roots $z = -1$ (light blue) and $z = 1$ (dark blue) as fixed points of the rational function (5), together with the probability $P_{-1}(m, n)$ for different multiplicities m and n .

Then, the resulting table for $P_1(m, n)$ can be also obtained by transposing rows and columns in the table above:

$$P_1(m, n) = P_{-1}(n, m).$$

Taking the sixth subdivision and a maximum number of iterations equal to 100, the values of probabilities $P_{-1}^{\text{M6}}(m, n)$ have been computed with *Mathematica* in Table 2. One can easily check that a precision of two decimal places is obtained. When we compare with the fifth subdivision, we have:

$$|P_{-1}^{\text{M5}}(m, n) - P_{-1}^{\text{M6}}(m, n)| < 4.8 \cdot 10^{-3}, \quad 1 \leq m, n \leq 8.$$

Remark 4. *The level of accuracy of these algorithms can be improved using finer subdivisions. For instance, for $m = 2$ and $n = 1$, taking a new subdivision Sd^7 , we obtain a better precision: $|P_{-1}^{\text{M6}}(2, 1) - P_{-1}^{\text{M7}}(2, 1)| < 1.2 \cdot 10^{-4}$. However, in our study we focus on the study of the influence of multiplicity more than on the analysis of the level of accuracy in the calculation of the probability.*

	$n = 1$	$n = 2$	$n = 3$	$n = 4$	$n = 5$	$n = 6$	$n = 7$	$n = 8$
$m = 1$	0.5	0.7659	0.8513	0.8883	0.9080	0.9285	0.9342	0.9466
$m = 2$	0.2341	0.5	0.6539	0.7402	0.7930	0.8283	0.8536	0.8715
$m = 3$	0.1487	0.3461	0.5	0.6054	0.6810	0.7310	0.7684	0.7966
$m = 4$	0.1117	0.2598	0.3946	0.5	0.5831	0.6430	0.6926	0.7298
$m = 5$	0.0920	0.2070	0.3190	0.4169	0.5	0.5641	0.6195	0.6620
$m = 6$	0.0715	0.1717	0.2690	0.3570	0.4359	0.5	0.5565	0.6014
$m = 7$	0.0658	0.1464	0.2317	0.3074	0.3805	0.4435	0.5	0.5448
$m = 8$	0.0534	0.1285	0.2034	0.2702	0.3380	0.3986	0.4552	0.5

Table 1: Probabilities $P_{-1}^{M5}(m, n)$ (related to the basin of $z = -1$) for different multiplicities m, n calculated with *Mathematica* by first projecting and then taking the fifth subdivision.

	$n = 1$	$n = 2$	$n = 3$	$n = 4$	$n = 5$	$n = 6$	$n = 7$	$n = 8$
$m = 1$	0.5	0.7665	0.8512	0.8898	0.9127	0.9259	0.9357	0.9447
$m = 2$	0.2335	0.5	0.6527	0.7402	0.7928	0.8287	0.8532	0.8711
$m = 3$	0.1488	0.3473	0.5	0.6060	0.6801	0.7325	0.7712	0.7989
$m = 4$	0.1102	0.2598	0.3940	0.5	0.5818	0.6445	0.6920	0.7284
$m = 5$	0.0873	0.2072	0.3199	0.4182	0.5	0.5667	0.6196	0.6632
$m = 6$	0.0741	0.1713	0.2675	0.3555	0.4333	0.5	0.5543	0.6018
$m = 7$	0.0643	0.1468	0.2288	0.3080	0.3804	0.4457	0.5	0.5480
$m = 8$	0.0553	0.1289	0.2011	0.2716	0.3368	0.3982	0.4520	0.5

Table 2: Probabilities $P_{-1}^{M6}(m, n)$ (related to the basin of $z = -1$) for different multiplicities m, n calculated with *Mathematica* by first projecting and then taking the sixth subdivision.

5.3 Comparing two different algorithms implemented in different computational environments

In Table 3, we have written the probability $P_{-1}^{S6}(m, n)$ obtained by the implementation in *Sage* of the algorithm referred in paragraph 4.2.1 (projection of the subdivisions) taking the sixth subdivision $\eta(\text{Sd}^6(\mathcal{S}))$. Observe that, although different strategies and programs have been used to estimate the probabilities $P_{-1}^{S6}(m, n)$ and $P_{-1}^{M6}(m, n)$,

$$|P_{-1}^{S6}(m, n) - P_{-1}^{M6}(m, n)| < 2.1 \cdot 10^{-3}, \quad 1 \leq m, n \leq 8;$$

that is, both processes provide similar results.

5.4 Quantification of the influence of multiplicity with potential and polynomial functions

In order to obtain a more precise quantification of the influence of multiplicities m and n on the probability related to the roots of the polynomial (4), we

	$n = 1$	$n = 2$	$n = 3$	$n = 4$	$n = 5$	$n = 6$	$n = 7$	$n = 8$
$m = 1$	0.5	0.7660	0.8502	0.8893	0.9114	0.9259	0.9360	0.9438
$m = 2$	0.2340	0.5	0.6538	0.7397	0.7927	0.8284	0.8526	0.8711
$m = 3$	0.1498	0.3462	0.5	0.6067	0.6805	0.7327	0.7702	0.7989
$m = 4$	0.1107	0.2603	0.3933	0.5	0.5814	0.6446	0.6921	0.7285
$m = 5$	0.0886	0.2073	0.3195	0.4186	0.5	0.5659	0.6193	0.6627
$m = 6$	0.0741	0.1716	0.2673	0.3554	0.4341	0.5	0.5563	0.6028
$m = 7$	0.0640	0.1474	0.2298	0.3079	0.3807	0.4437	0.5	0.5478
$m = 8$	0.0562	0.1289	0.2011	0.2715	0.3373	0.3972	0.4522	0.5

Table 3: Probabilities $P_{-1}^{S_6}(m, n)$ (related to the basin of $z = -1$) for different multiplicities m, n calculated with *Sage* by first taking the sixth subdivision and then projecting.

n	$P_{-1}^{M_6}(m, n)$	R^2
1	$0.4872m^{-1.0547}$	0.9987
2	$1.0099m^{-0.9876}$	0.9987
3	$1.4223m^{-0.9358}$	0.9979
4	$1.7165m^{-0.883}$	0.9986
5	$1.9384m^{-0.8391}$	0.9989

Table 4: Potential approach to $P_{-1}^{M_6}(m, n)$ for $m \geq n$ and a fixed n .

show in Table 4 and Table 5 functions that are rather good approximations of $P_{-1}(m, n)$, in the first case for a fixed n and in the second case for a fixed m . These approximations have been calculated by means of the method of least squares. In both tables, the value R^2 represents the coefficient of determination, which measures the goodness-of-fit.

For each fixed $n \in [1, 5]$, a graphic of the original probabilities $P_{-1}^{M_6}(m, n)$ and the corresponding potential fitting functions can be seen in Figure 6. In the same way, another plot of these probabilities for $4 \leq m \leq 8$ and their relative polynomial fitting functions is shown in Figure 7.

Remark 5. Note that Newton's method can also be applied when the multi-

m	$P_{-1}^{M_6}(m, n)$	R^2
8	$-0.0022n^2 + 0.084n - 0.0287$	0.9999
7	$-0.0028n^2 + 0.0961n - 0.0315$	0.9998
6	$-0.004n^2 + 0.1141n - 0.0377$	0.9999
5	$-0.0065n^2 + 0.1425n - 0.0497$	0.9999
4	$-0.0109n^2 + 0.1849n - 0.0644$	0.9999

Table 5: Polynomial approach to $P_{-1}^{M_6}(m, n)$ for $m \geq n$ and a fixed m .

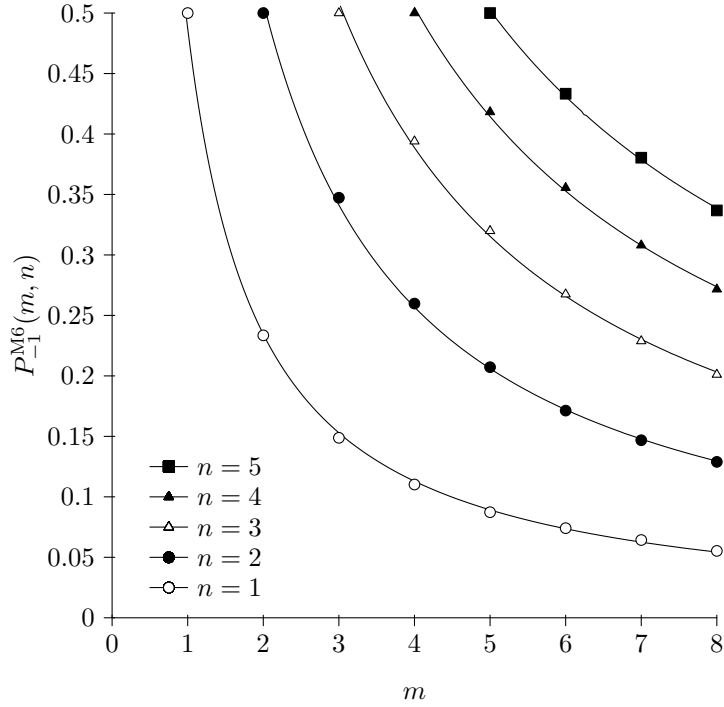


Figure 6: Values of the probabilities $P_{-1}^{M6}(m, n)$ when the lowest multiplicity n is fixed.

probabilities m, n are not integers. Even more, the algorithms described in this paper also work in this case and the potential and polynomial functions given in Table 4 and Table 5 give a good approximation to the probability when one of the two multiplicities is an integer. For instance, let us consider the case $n = 2$. The potential function obtained from Table 4 (see also Figure 6) for $n = 2$ is denoted by $g_2(m) = 1.0099m^{-0.9876}$. The following pairs give the values of $P_{-1}^{M6}(m, 2)$ and its approximations by $g_2(m)$ for different not necessarily integer values of m :

$$\begin{aligned}
 P_{-1}^{M6}(5, 2) &= 0.2072, g_2(5) = 0.2060; & P_{-1}^{M6}(5.2, 2) &= 0.1988, g_2(5.2) = 0.1982; \\
 P_{-1}^{M6}(5.4, 2) &= 0.1916, g_2(5.4) = 0.1909; & P_{-1}^{M6}(5.6, 2) &= 0.1853, g_2(5.6) = 0.1842; \\
 P_{-1}^{M6}(5.8, 2) &= 0.1777, g_2(5.8) = 0.1779; & P_{-1}^{M6}(6, 2) &= 0.1713, g_2(6) = 0.1720.
 \end{aligned}$$

Similar observations can be done for the functions of Table 5 plotted in Figure 7.

Remark 6. The graphics shown in Figure 6 suggest that, for a fixed n , the probability $P_{-1}^{M6}(m, n) \rightarrow 0$ when $m \rightarrow +\infty$. Note that, for multiple roots, the rational functions given by Newton's method has always quadratic degree. For this reason, in this case we can avoid the problem of working with rational functions of high degree that appears when Newton's method is applied to a

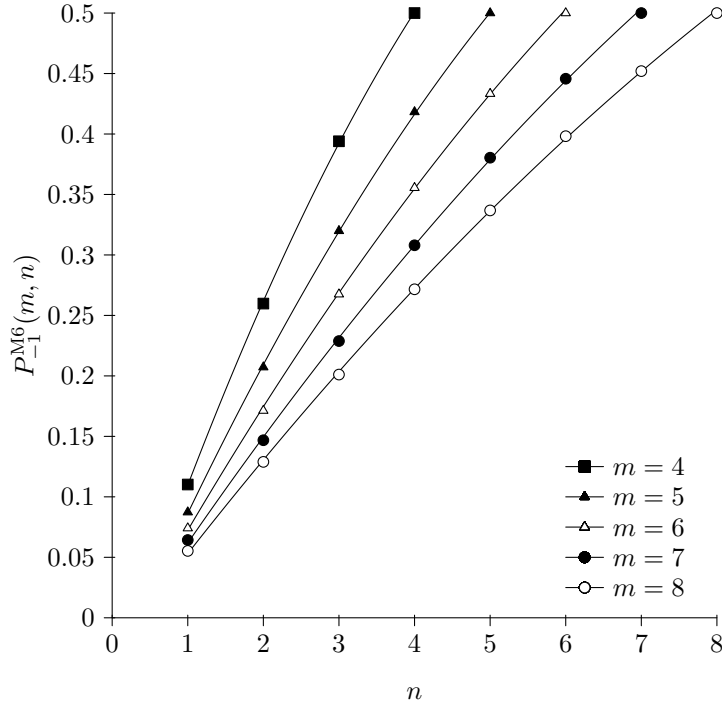


Figure 7: Values of the probabilities $P_{-1}^{M6}(m, n)$ when the highest multiplicity m is fixed.

high order polynomial with simple roots. We have checked the goodness of fit of the calculations performed for $n = 2$ and higher values of m , in particular, $m = 10, 20, 30$. In these cases, the values of the potential function given in Table 4 for $n = 2$, that is $g_2(m) = 1.0099m^{-0.9876}$, are:

$$g_2(10) = 0.103915, g_2(20) = 0.052406, g_2(30) = 0.0351134,$$

whereas the values of the probabilities obtained by our algorithms are

$$P_{-1}^{M6}(10, 2) = 0.104219, P_{-1}^{M6}(20, 2) = 0.0532655, P_{-1}^{M6}(30, 2) = 0.0375119.$$

As we can see, the corresponding values are quite similar. This fact suggests that the potential functions also give a good approximation when m tends to infinity. Consequently, the probability of reaching the root with lower multiplicity decreases to 0 when the multiplicity of the other root goes to infinity.

On the other hand, note that the functions defined in Table 5, whose graphics are given in Figure 7, are polynomials of degree 2. From these graphics, one could infer that in general for a fixed m , and for $1 \leq n \leq m$, the discrete function $P_{-1}^{M6}(m, n)$ can be approached by quadratic polynomials. In Figure 7, we also observe that, for $m = n$, one obtains $P_{-1}^{M6}(m, n) = 0.5$, as we have

already mentioned. This idea is supported by the result previously obtained in [17].

We can summarize saying that the discrete function $P_{-1}^{M6}(m, n)$, whose values are numerically given by our algorithms, can be approached, for a fixed n , by potential functions with (negative) non-integer exponents. In the same way, for a fixed m , the corresponding discrete function with domain $\{1, \dots, m\}$ is approached by a polynomial of degree 2.

Remark 7. One interesting question is to study the change of the probability of reaching a root when we consider different numerical methods. For instance, we have also made some experiments when the relaxed Newton's method

$$z_{n+1} = R_{p,\lambda}(z_n) = z_n - \lambda \frac{p(z_n)}{p'(z_n)}, \quad (6)$$

is applied to the polynomial $p(z) = (z - 1)^3(z + 1)^2$. In particular, we have chosen the values $\lambda = 2$ and $\lambda = 3$ for the relaxing parameter. Let us consider the root $z = -1$ and let us denote $P_{-1}^{R_{p,3}}(3, 2)$, and $P_{-1}^{R_{p,2}}(3, 2)$ the probabilities of reaching the root $z = -1$ by the relaxed Newton's method for $\lambda = 3$ and $\lambda = 2$, respectively. $P_{-1}^{N_p}(3, 2)$ denotes the probability obtained for Newton's method (given in Table 2). Then we have

$$P_{-1}^{R_{p,3}}(3, 2) = 0.2842 < P_{-1}^{R_{p,2}}(3, 2) = 0.3250 < P_{-1}^{N_p}(3, 2) = 0.3473.$$

In our opinion, the behavior of the probability of reaching a given root using different generalized Newton's methods should be analyzed in a more detail in future works using more numerical calculi and new simulations. We are aware that for generalized Newton's method there are other factors that must be taken into account to analyze the structure of the related Julia sets, such as the existence of extraneous fixed points (see Ref. [12]).

6 Conclusions and further work

In this paper, we have developed two algorithms to measure the basins of attraction of the fixed points of a rational function in the Riemann sphere. We have used two different mathematical programs in order to implement them. Actually, one of them has been implemented with *Sage* and the other one with *Mathematica*. As an application, we have measured the basins of attraction of the fixed points of the rational function obtained when Newton's method is applied to a polynomial in the form (4). Note that this fixed points are the roots $\alpha_1 = -1$ and $\alpha_2 = 1$ of such polynomial. Next, we have assigned probabilities $P_{-1}(m, n)$ and $P_1(m, n)$ to the roots depending on their multiplicities (m, n) with the following criterium: $P_{\alpha_i}(m, n)$ denotes the probability for a point in the Riemann sphere to belong to the basin of attraction of α_i , $i = 1, 2$.

We have written this paper with the aim of connecting to different theories, such as the numerical solution of nonlinear equations and the dynamics of some

topological spaces. We are aware that there are many other questions that could be taken into account in further works. For instance, we think that it would be worthy to complete our initial numerical experiments with, at least, the following aspects:

- (i) Analysis of the probabilities $P_{\alpha_i}(m, n)$ and their properties for other choices of the roots and not only for two opposite unitary roots $-\alpha_1 = \alpha_2 = 1$.
- (ii) Generalization to polynomials with three or more roots and their corresponding multiplicities.
- (iii) Comparison of the influence of multiplicity on the measure of basins of attraction when other numerical methods are considered: relaxed Newton's method, Chebyshev's method, Halley's method, etc. In this way, it would be interesting to take into account previous results obtained for these methods in the references [11] or [14], for instance.
- (iv) Application of our algorithms for iteration functions not necessary rational, such as complex exponential functions, trigonometric functions, etc. The references [15] and [16] could be very helpful in this way.
- (v) Development of some algorithms to evaluate the length of the Julia set in the Riemann sphere.
- (vi) Search and implementation of new measure algorithms based on a spherical subdivision in quadrilaterals with the same area. In our opinion, this fact would improve the efficiency of the algorithms.
- (vii) Development of new measure algorithms based on subdivision of other regular polyhedra; for instance, the icosahedron or other spherical subdivisions with adequate dispersion and discrepancy (see [6, 18]).

Of course, this list could be extended with many other questions, such as a local consideration of the probability with the standard measure of \mathbb{C} or a statistical analysis of the problem.

From a topological point of view, it would be interesting to study some topological and shape invariants either of the Julia set or of the basins of rational maps. For instance, cubical structures and consecutive subdivisions are canonical tools that can be used to compute these invariants.

Trying to find a representative sample on the sphere in order to study probability phenomena is a well-known problem. This question is strongly related to the study of astronomical data distributed on the entire sky. In some cases it is only necessary to cover a partial area corresponding to a galactic object. The use of cubical structures of the sphere and measure procedures is a very useful technique in Astronomy and Astrophysics. The fractal geometry of these data gives interesting methods for the study of astrophysics phenomena. The satellite observation of the cosmos can be organized using cellular and cubical decomposition of the 2-sphere and modifications of the algorithms developed in

this work can be useful in the study of astronomical data. Similar conclusions can be obtained when one tries to analyze geological data given by observation satellites, specifically designed to observe Earth from orbit for uses such as environmental monitoring, meteorology, map making etc. There are other possible application fields as, for instance, the study of spherical viruses or spherical fullerene structures, etc.

References

- [1] S. Amat, S. Busquier and S. Plaza, *Review of some iterative root-finding methods from a dynamical point of view*, Scientia, Ser. A Math. Sci., vol. 10, 3–35 (2004).
- [2] I. K. Argyros, *Convergence and Applications of Newton-Type Iterations*, Springer, 2008.
- [3] A. F. Beardon, *Iteration of Rational Functions*, Springer-Verlag, 2000.
- [4] J. M. García-Calcines, L. J. Hernández and M. T. Rivas, *Limit and end functors of dynamical systems via exterior spaces*, To appear in Bulletin of the Belgium Math. Soc.- Simon Stevin, vol. 21, (2014).
- [5] W. J. Gilbert, *The complex dynamics of Newton's method for a double root*, Computers Math. Applic., vol. 22, no. 10, 115–119 (1991).
- [6] K. M. Górski, E. Hivon, A. J. Banday, B. D. Wandelt, F. K. Hansen, M. Reinecke and M. Bartelman, *HEALPix – a Framework for High Resolution Discretization, and Fast Analysis of Data Distributed on the Sphere*, Astrophys. J., vol. 622, 759–771 (2005).
- [7] L. J. Hernández, M. Marañón and M. T. Rivas, *Plotting basins of end points of rational maps with Sage*, Tbilisi Math. J., vol. 5, no. 2, 71–99 (2012).
- [8] H. O. Peitgen, H. Jürgens and D. Saupe, *Cayley's problem and Julia sets*, Math. Intelligencer, vol. 6, no. 2, 11–20 (1984).
- [9] J. F. Traub, *Iterative Methods for the Solution of Equations*, Prentice-Hall, 1964.
- [10] J. L. Varona, *Graphic and numerical comparison between iterative methods*, Math. Intelligencer, vol. 24, no. 1, 37–46 (2002).
- [11] Wang Xingyuan and Liu Bo, *Julia sets of the Schröder iteration functions of a class of one-parameter polynomials with high degree*, Appl. Math. Comput., vol. 178, no. 2, 461–473 (2006).
- [12] Wang Xingyuan and Tingting Wang, *Julia sets of generalized Newton's method*, Fractals, vol. 15, no. 4, 323–336 (2007).

- [13] Wang Xingyuan and Liu Wei, *The Julia set of Newton's method for multiple root*, Appl. Math. Comput., vol. 172, no. 1, 101–110 (2006).
- [14] Wang Xingyuan and Yu Xuejing, *Julia sets for the standard Newton's method, Halley's method, and Schröder's method*, Appl. Math. Comput., vol. 189, no. 2, 1186–1195 (2007).
- [15] Wang Xingyuan and Yu Xuejing, *Julia set of the Newton transformation for solving some complex exponential equation*, Fractals, vol.17, no. 2, 197–204 (2009).
- [16] Wang Xingyuan, Yi-Ke Li, Yuan-Yuan Sun, Jun-Mei Song and Feng-Dan Ge, *Julia sets of Newton's method for a class of complex-exponential function $F(z) = P(z)e^{Q(z)}$* , Nonlinear Dynamics, vol. 62, no. 4, 955–966 (2010).
- [17] W. Yang, *Symmetries in the Julia sets of Newton's method for multiple roots*, Appl. Math. Comput., vol. 217, 2490–2494 (2010).
- [18] A. Yershova, S. Jain, S. M. LaValle, and J. C. Mitchell, *Generating Uniform Incremental Grids on $SO(3)$ using the Hopf Fibration*, International Journal of Robotics Research, vol. 29, no. 7, 801–812 (2010).